Anisotropy of acceleration in turbulent flows

A. M. Reynolds,[1,*] K. Yeo,[2] and C. Lee[2]
[1]*Silsoe Research Institute, Wrest Park, Silsoe, Bedford, MK45 4HS, United Kingdom*
[2]*Department of Mechanical Engineering, Yonsei University, 134 Shinchon-dong, Seodaemun-gu, Seoul, 120-749, Korea*
(Received 12 January 2004; published 9 July 2004)

Third-order Lagrangian stochastic models for the evolution of fluid-particle hyperaccelerations (material derivatives of Lagrangian accelerations) are shown to account naturally for the anisotropy of acceleration variances in low-Reynolds-number turbulent flows and for their dependency upon the energy-containing scales of motion. Model predictions are shown to be in close accord with the results of direct numerical simulations for a turbulent channel flow and with previously acquired simulation data for a homogeneous turbulent shear flow.

DOI: 10.1103/PhysRevE.70.017302 PACS number(s): 47.27.Eq, 02.50.Ey, 05.10.Gg, 05.20.Jj

I. INTRODUCTION

According to Kolmogorov's similarity theory, at very large Reynolds numbers the acceleration variance is isotropic and prescribed by $\sigma_A^2 = a_0 \epsilon^{3/2} \nu^{-1/2}$, where a_0 is a universal constant, ϵ is the mean rate of dissipation of turbulent kinetic energy divided by the fluid density, and ν is the kinematic viscosity. The results of direct numerical simulations (DNSs) of turbulent channel flow described here and laboratory-scale experiments [1–4] indicate that acceleration variances are dependent upon Reynolds number and are decidedly anisotropic. Here, it is demonstrated that departures from universality and isotropy observed in low-Reynolds-number turbulence can be attributed to the influence of hyperaccelerations (the material derivative of the acceleration) and that compatibility with Kolmogorov similarity scaling can be "restored" when hyperaccelerations are accounted for explicitly. Inferences about the observed anisotropy of acceleration variances in high-Reynolds-number turbulence are also made. This is done within the context of a third-order Lagrangian stochastic (LS) model [5]. In addition to the time scales T_L and t_η introduced at second order and pertaining to the "energy-containing" and "dissipative" scales of motion, third-order models contain a third time scale t_3. This additional time scale results in a finite hyperacceleration variance $\sigma_{\mathring{A}}^2$ and renders simulated Lagrangian accelerations continuous and differentiable. Hyperaccelerations are correlated exponentially on a time scale t_3 when $t_3 \ll t_\eta \ll T_L$. The findings have important ramifications for more conventional Lagrangian stochastic models based on first- and second-order truncations because they illustrate that the apparent nonuniversality of a_0 attained in such models [6] is not an intrinsic shortcoming of the approach in general but a consequence of truncation. A prescription for effective model parameters that accounts for neglected third-order processes follows directly from the evaluation of third-order processes presented below.

II. THIRD-ORDER EFFECTS IN TURBULENT FLOWS AT LOW REYNOLDS NUMBERS

The simplest third-order LS model for the evolution of hyperaccelerations $\mathring{A}$ in homogeneous anisotropic turbulence is prescribed by

$$\begin{aligned} d\mathring{A}_i &= (a_{ij} + c_{ij})\mathring{A}_j dt + (b_{ij} - c_{ik}a_{kj})A_j dt - c_{ik}b_{kj}u_j dt \\ &\quad + \sqrt{-2(a_{ij} + c_{ij})\lambda_{jk}}\, d\xi_k, \\ dA_i &= \mathring{A}_i dt, \\ du_i &= A_i dt, \end{aligned} \tag{1}$$

where

$$\begin{aligned} a_{ij} &= -C_0 \epsilon \tau_{ij} - \frac{2a_0}{C_0}\epsilon^{1/2}\nu^{-1/2}\delta_{ij}, \\ b_{ij} &= -a_0 \epsilon^{3/2}\nu^{-1/2}\tau_{ij}, \\ c_{ij}(\chi_{jk} + b_{jl}\sigma_{lk}) &= -a_{ij}\chi_{jk}. \end{aligned}$$

A is the Lagrangian acceleration, u is the Lagrangian velocity, $\tau_{ij} = [\sigma^{-1}]_{ij}$, $\sigma_{ij} = \langle u_i u_j \rangle$, $\chi_{ij} = \langle A_i A_j \rangle$, $\lambda_{ij} = \langle \mathring{A}_i \mathring{A}_j \rangle$, C_0 is Kolmogorov's constant for the Lagrangian velocity structure function, and $d\xi_i$ are increments of independent Weiner processes with mean zero and variance dt [5]. By construction, the velocity, acceleration, and hyperacceleration statistics are jointly Gaussian, and when the inverse time scales associated with the third-order processes $c_{ij \to \infty}$, the acceleration variances are prescribed by Kolmogorov similarity scaling; $\sigma_A{}^2 = a_0 \epsilon^{3/2}\nu^{-1/2}$. In the limit that the inverse time scales $c_{ij \to \infty}$, hyperaccelerations become uncorrelated, hyperacceleration variances $\lambda_{ij \to \infty}$, and Eq. (1) reduces to the second-order LS model,

$$dA_i = a_{ij}A_j dt + b_{ij}u_j dt + \sqrt{-2a_{ij}\chi_{jk}}\, d\xi_k. \tag{2}$$

The potential of the third-order modeling approach is now illustrated by comparing model predictions with the results of DNSs acquired for a turbulent channel flow with $R_\lambda \sim 30$ where R_λ is the Reynolds number based upon the Taylor microscale $\lambda = (15\nu\sigma_u^2/\epsilon)$. This Eulerian Reynolds number corresponds to a Lagrangian Reynolds number $\mathrm{Re}_* = (T_L/t_\eta)^2 \sim 5$. The turbulent channel flow was simulated using a spectral method incorporating Fourier expansions in the homogeneous horizontal directions and Chebyshev expansions in the wall-normal directions. The computational domain was $(4\pi, 2, 4\pi/3)h$ and contained 128^3 grid cells, where h is the channel half-width. A third-order Runge-Kutta scheme combined with the Crank-Nicolson scheme was used to advance time. A particle tracking algorithm employing the four-point Hermite interpolation in the horizontal directions

*Author to whom correspondence should be addressed. FAX: +44 (0)1525 860156. Email address: andy.reynolds@bbsrc.ac.uk

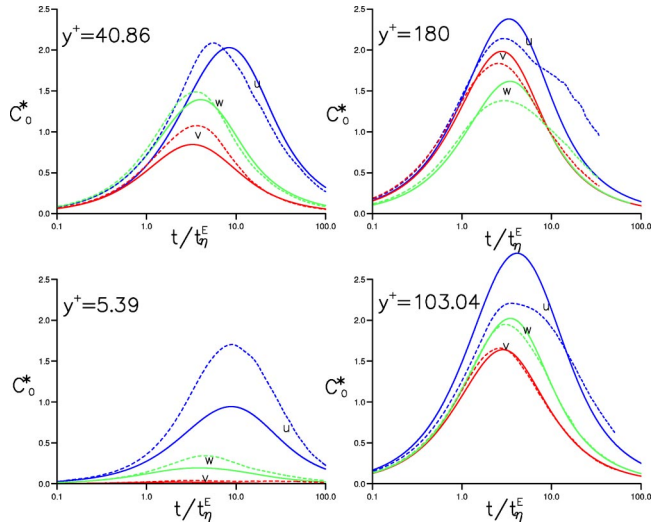

FIG. 1. (Color online) DNS data for the approach of the Lagrangian velocity structure function to inertial subrange behavior in a turbulent channel flow with nondimensional height $hu_*/\nu \equiv h^\dagger = 180$, where ν is the kinematic viscosity and u_* is the friction velocity (dashed lines). The lines pass smoothly through data points acquired at $0.032 t_\eta^E$ intervals. Predictions obtained using a third-order LS model with $C_0=6$ and $a_0=5.5$ are also shown (solid lines). The nondimensional height y^+ of the origin of the trajectories is indicated. The letter adjacent to the pairs of curves denotes the velocity component.

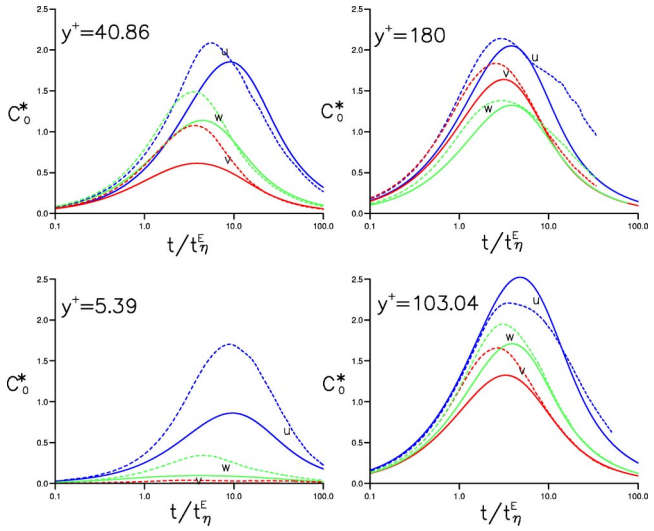

FIG. 2. (Color online) DNS data for the approach of the Lagrangian velocity structure function to inertial subrange behavior in a turbulent shear flow with nondimensional height $hu_*/\nu \equiv h^\dagger = 180$, where ν is the kinematic viscosity and u_* is the friction velocity (dashed lines). The lines pass smoothly through data points acquired at $0.032\ t_\eta^E$ intervals. Predictions obtained using a second-order LS model with $C_0=6$ and nonuniversal anisotropic values of a_0 calculated using the Kolmogorov similarity scaling relation $a_0 = \sigma_A^2 \epsilon^{-3/2} \nu^{1/2}$, and the results of DNS are also shown (lines: streamwise, solid line; vertical, dotted line; cross wind, dashed line). The nondimensional height $y^\dagger$ of the origin of the trajectories is indicated. The letter adjacent to the pairs of curves denotes the velocity component.

and Chebyshev interpolation in the wall-normal direction was used to obtain Lagrangian statistics along fluid particle trajectories. Further details about the DNS and particle tracking algorithm can be found in the recent paper of Choi *et al.* [7].

Estimates for the value of a_0 obtained from the DNS data for the three components of acceleration (streamwise, cross wind, and vertical), under the assumption that $\sigma_A^2 = a_0 \epsilon^{3/2} \nu^{-1/2}$, range from about (0.29, 0.03, 0.15) at the top of the viscous layer to about (1.67, 1.57, 1.05) at the center of the channel. Figure 1 shows that estimates for the value of C_0 obtained from the Lagrangian velocity structure function $D(t)_{ii} = \langle [u_i(t+\tau) - u_i(t)]^2 \rangle$ (no summation) are also decidedly anisotropic and nonuniversal. According to Kolmogorov scaling, at very large Reynolds numbers and for inertial subrange times, a plot of $D(t)\epsilon t$ should show a plateau at height C_0.

The maxima in $D(t)/\epsilon t$ (denoted by C_0^*) are seen in Fig. 1 to occur at times comparable with the dissipation time scale. At these time scales, the influence of inhomogeneities in the statistical properties of the flow is of secondary importance in determining Lagrangian properties, i.e, changes in the statistical properties of the flow along trajectories of such short duration are not significant. Of greater importance are the statistics of the flow at the origin of the trajectories and the temporal correlations. These key quantities are incorporated into three-dimensional (3D) LS models for anisotropic homogeneous turbulence, like Eq. (1). The third-order model (1) can therefore be utilized to assess the extent to which hyperaccelerations account for the departures from Kolmogorov similarity scaling observed in a DNS.

The utilization of Eq. (1) in this manner requires estimates for C_0, a_0, and t_3. Here, in accordance with the only two reliable estimates for C_0 [8] and with recent experimental estimates for the asymptotic value of a_0 [3–9], we choose $C_0=6$ and $a_0=5.5$. The hyperacceleration variances were subsequently chosen to guarantee consistency with the DNS data for the acceleration variances. Model predictions for the hyperaccelerations were anisotropic and consistent (to within a factor of about 2 or less) with estimates for the hyperacceleration variance obtained from the DNS data for the Lagrangian acceleration autocorrelation function ρ using the kinematic relation $\sigma_A^2 = -\sigma_A^2 d^2\rho/dt^2|_{t=0}$. Just above the viscous layer, $t_3 > T_L > t_\eta$, while at the center of the channel $T_L > t_3 > t_\eta$. This lack of scale separation between second- and third-order processes has important implications for the correct parametrization of second-order LS models. This is because the parametrization of second-order processes (accelerations) in terms of Kolmogorov similarity theory for high-Reynolds-number turbulence is strictly justifiable only when $t_\eta \ll t_3$. Justification for the adoption of third-order models is dependent on there being a scale separation between third- and fourth-order processes. Although the ratio t_3/t_η was found to decrease with increasing Reynolds number R_λ, it is not possible with the current data to determine whether or not $t_3/t_\eta \to 0$ as $R_\lambda \to \infty$. If $t_3/t_\eta \to 0$ as $R_\lambda \to \infty$ then Kolmogorov scaling of the acceleration variance is recovered at high Reynolds number. If t_3/t_n tends to a finite value then hyperacceleration statistics may account for the observed an-

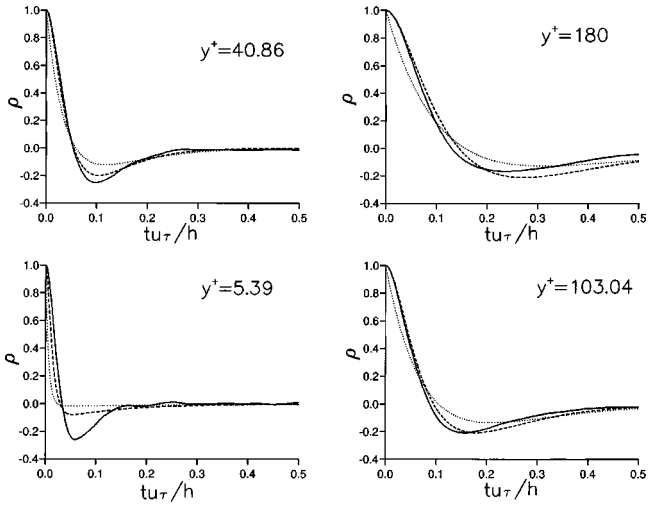

FIG. 3. DNS data (solid lines) and model predictions (second-order model, dotted line; third-order model, dashed line) for the Lagrangian acceleration autocorrelation function $\rho_{33}=\langle A_3(0)A_3(t)\rangle$ (lateral direction). For the second-order model, predictions are shown for $C_0=6$ and nonuniversal anisotropic values of a_0 calculated using the Kolmogorov similarity scaling relation $a_0=\sigma_A^2\epsilon^{-3/2}\nu^{1/2}$, and the results of DNS. For the third-order model, predictions are shown for $C_0=6$ and $a_0=5.5$. Time has been nondimensionalized using the friction velocity u_τ and the height of the boundary layer h. The nondimensional height $y^\dagger$ of the origin of the trajectories is indicated.

isotropy of acceleration variances in high-Reynolds-number turbulence [3,9]. This is most evident for the case when velocity and acceleration covariances vanish so that model (1) reduces to three decoupled 1D models. The time scales in the 1 D models, $T_L=2\sigma_u^2/C_0\epsilon$, $t_\eta=(C_0/2a_0)(\nu/\epsilon)^{1/2}$, $t_3=c_{11}^{-1}$, etc., are related to the velocity, acceleration, and hyperacceleration variances by

$$\sigma_A^2=\frac{\sigma_u^2}{T_L t_\eta+T_L t_3+t_\eta t_3},$$

$$\sigma_{\dot{A}}^2=\sigma_A^2(T_L^{-1}t_\eta^{-1}+T_L^{-1}t_3^{-1}+t_\eta^{-1}t_3^{-1}). \tag{3}$$

It is apparent from Eq. (3) that when $t_3=0$ (as it is in second-order LS models), $\sigma_A^2=\sigma_u^2/T_L t_\eta=a_0\epsilon^{3/2}\nu^{-1/2}$, in accordance with Kolmogorov's similarity theory, and that consequently anisotropy of σ_A^2 implies anisotropy of a_0. This is not necessarily the case when $t_3\neq 0$. When $t_3\neq 0$, σ_A^2 will in general be dependent upon σ_u^2 and so dependent upon the "energy-containing" scales of motion.

Figure 1 illustrates that the third-order model (1) reproduces accurately the approach toward inertial subrange scaling attained in the results of DNSs for locations well above a viscous sublayer that extends to a nondimensional height $y^\dagger=yu_*/\nu=5$ where u_* is the friction velocity. The discrepancy between the model predictions and the DNS data that is evident just above the viscous sublayer may be due to the effects of coherent flow structures which have not been incorporated into the model. The tendency of the model to overpredict values of C_0 corresponding to the streamwise component of velocity could be due to the neglect of the influence of rotations of the Lagrangian velocity vector in-

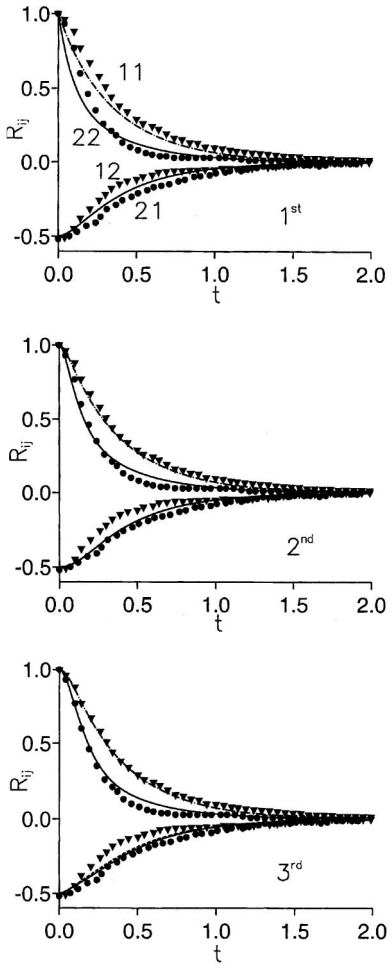

FIG. 4. Normalized Lagrangian velocity autocorrelation functions $R_{ij}=\langle u_i(0)u_j(s)\rangle/(\sigma_{ii}\sigma_{jj})^{1/2}$ (no summation; 1, streamwise direction, 2, vertical direction) for homogeneous turbulent shear flow. DNS data (symbols) and model predictions (lines) obtained using first-, second-, and third-order models with $C_0=6$ and $a_0=5.5$.

duced by the mean shear. Figure 2 shows that the DNS data are represented less satisfactorily by the second-order model (2) with $C_0=6$, despite the effective employment of nonuniversal anisotropic values for a_0. Moreover, it is evident that unrealistically large values of $C_0^*(C_0>6)$ are required to match the peak values of C_0^* attained in the DNS. Figure 3 shows that, except for close to the viscous sublayer, predictions for the Lagrangian acceleration autocorrelation function obtained using the third-order model are in close agreement with DNS data. This is particularly evident at short times, where model predictions and DNS data for the gradients in the Lagrangian acceleration autocorrelation function (and consequently the hyperacceleration variances) are seen to be very nearly coincident.

Pope [6,10] recently undertook a detailed analysis of first- and second-order LS models for simulating fluid-particle trajectories in homogeneous turbulent shear flow. He established a one-to-one correspondence between model coefficients and primary flow statistics, such as the velocity variances and integral Lagrangian times scales. The model agreement with the results of DNSs [11,12] was excellent but

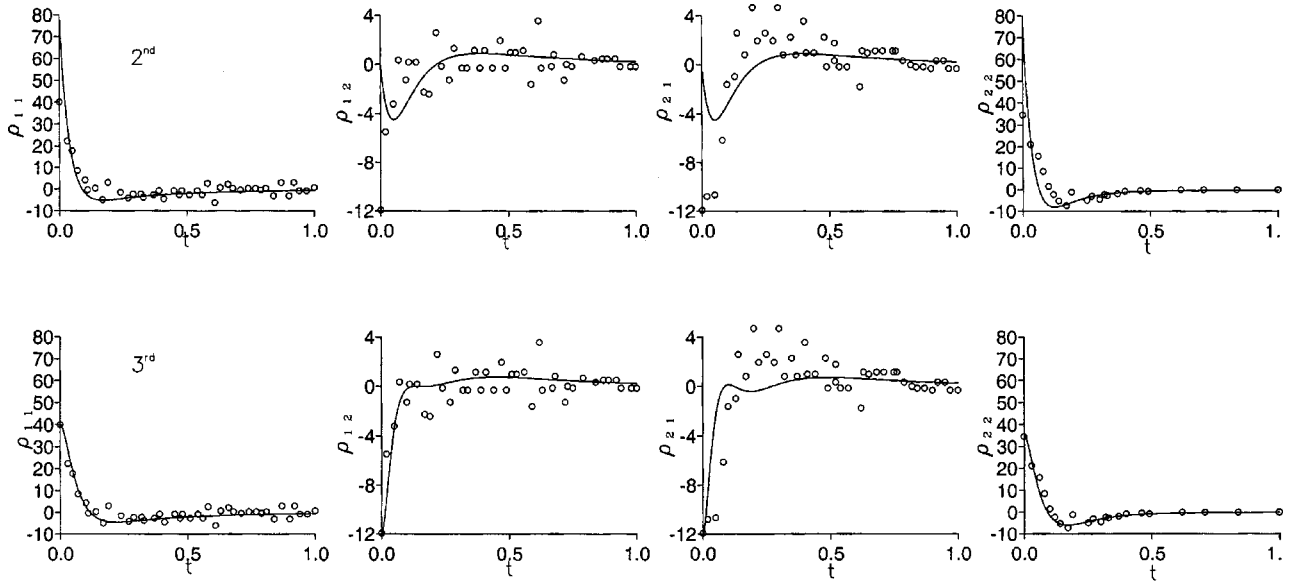

FIG. 5. Lagrangian acceleration autocorrelation functions $\rho_{22}=\langle A_2(0)A_2(t)\rangle$ (1, streamwise direction; 2, vertical direction) for homogeneous turbulent shear flow. DNS data (symbols) and model predictions (lines) obtained using second-(upper) and third- (lower) order models with $C_0=6$ and $a_0=5.5$.

the supposed universality of C_0 and a_0 was not respected. Here, it is demonstrated that this deficiency is overcome in third-order formulations.

The results of DNSs reveal that after an initial transient homogeneous turbulent shear flow tends to an approximately self-similar state in which quantities pertaining to the energy-containing scales (velocity, velocity variances, dissipation) are approximately constant, when normalized by the turbulent kinetic energy k and ϵ. Complete stationarity is not attained because the Reynolds number $k^2/(\epsilon\nu)$ increases with time. Departures from nonstationarity are, however, small and consequently homogeneous turbulent shear flow can, to a good approximation, be treated as stationary anisotropic turbulence. Indeed, over the time interval of the DNS, the modulus of $\mathbf{A}$ increases by approximately 10%, while the Kolmogorov dissipation time scale decreases by about 20% [6]. Sawford and Yeung [11,12] did not report on λ_{ij} and here our values are chosen to guarantee consistency with the DNS data for χ_{ij} while retaining $C_0=6$ and $a_0=5.5$.

Figures 4 and 5 reveal that predictions for the Lagrangian velocity autocorrelation functions and the Lagrangian acceleration autocorrelation functions obtained using the third-order model are in excellent agreement with the DNS data and significantly better than those obtained using first- and second-order models. The small difference between the predictions of the third-order model and the DNS data for the cross-velocity autocorrelation function ρ_{12} may indicate that on integral time scales the effect of rotation of trajectories due to shear needs to be accounted for explicitly. [13] It is worth emphasizing that the ability of the second-order model to accurately predict Lagrangian velocity autocorrelation functions is not mirrored by an ability to accurately predict second-order quantities. This is evident from Fig. 5, which shows that acceleration variances are overpredicted by a factor of about 2 by the second-order model while predictions for the acceleration covariances have the wrong sign.

III. SUMMARY

In this paper, third-order processes have been shown to account naturally for the anisotropy of Lagrangian accelerations observed in DNS data for turbulence at low Reynolds number. The apparent nonuniversality of parameters in conventional Lagrangian stochastic models was shown to be a consequence of truncation at either first or second order and not an inherent deficiency of the approach in general. Analysis of third-order processes provides a prescription for a reparametrization of these more conventional models and provides us with greater confidence in their "correctness" and in truncation at second order, in particular.

[1] S. Kurien and S. Sreenivasan, Phys. Rev. E **62**, 2206 (2000).
[2] X. Shen and Z. Warhaft, Phys. Fluids **12**, 2976 (2000).
[3] A. La Porta, G. A. Voth, A. M. Crawford, J. Alexander, and E. Bodenschatz, Nature (London) **409**, 1017 (2001).
[4] G. A. Voth, A. La Porta, A. M. Crawford, J. Alexander, and E. Bodenschatz, J. Fluid Mech. **469**, 121 (2002).
[5] A. M. Reynolds, Phys. Fluids **15**, 2773 (2003).
[6] S. B. Pope, Phys. Fluids **14**, 2360 (2002).
[7] J. I. Choi, K. Yeo, and C. Lee, Phys. Fluids **16**, 779 (2004).
[8] R-C. Lien and E. A. D'Asaro, Phys. Fluids **14**, 4456 (2002).
[9] G. A. Voth, K. Satyanarayan, and E. Bodenschatz, Phys. Fluids **10**, 2268 (1998).
[10] S. B. Pope, Phys. Fluids **14**, 1696 (2002).
[11] B. L. Sawford and P. K. Yeung, Phys. Fluids **12**, 2033 (2000).
[12] B. L. Sawford and P. K. Yeung, Phys. Fluids **13**, 2627 (2001).
[13] B. L. Sawford (private communication).